Effect of Varying *Cinnamomum camphora* Leaf Powder Content on the Pelletizing Quality of Bamboo Fiber Biomass Pellets for Renewable Energy Applications

Yunjie Xu, Xinghua Ye, Xun Guan,* Liang Zhang, and Xiaojun Hu

Addressing the issue of low effective utilization of moso bamboo in Zhejiang Province, this study investigated the impact of varying camphor leaf powder content on the granulation quality of bamboo fiber biomass pellets, using moso bamboo fibers and camphor tree leaves from Zhejiang as raw materials. Experimental analysis examined moisture content, mixing ratio, and molding pressure effects on pellet density and mechanical durability. The experimental results revealed that under the same conditions, the performance of bamboo fiber pellets without camphor leaf powder is significantly inferior to those containing camphor leaf powder. As moisture content rose from 3% to 9%, pellet density and durability increased, but further increases to 18% led to their decline. Orthogonal experiments demonstrated that both moisture content and molding pressure had significant effects on density and mechanical durability. The calorific value test results indicated that the higher heating value of the mixed pellets reached 4380 Kcal/kg. The findings of this study provide insights for enhancing the utilization efficiency of moso bamboo and camphor tree leaf resources.

DOI: 10.15376/biores.19.4.7080-7101

Keywords: Moso bamboo fiber; Camphor leaf; Moisture content; Density; Mechanical durability

Contact information: School of Engineering, Huzhou University, Huzhou 313000, China;

* Corresponding author: guanxun@zjhu.edu.cn

INTRODUCTION

Since the 21st century began, there has been a significant increase in demand for non-renewable energy sources such as fossil fuels. However, the growing concerns over the non-renewability of fossil fuels and their environmental impacts have put traditional energy sources under pressure (Lin and Xu 2020; Olabi *et al.* 2022). There is an urgent need to seek renewable alternatives. Biomass energy, increasingly valued for its environmental friendliness and renewability, stands out as one such viable option (Yana *et al.* 2022; Zastempowski 2023).

Biomass energy, produced through photosynthesis, involves the systematic processing and efficient utilization of resources, such as residual forest biomass, crop residues, and livestock excreta. These resources can be converted into a range of energy forms, including electricity, heat, biogas, as well as synthetic fuels such as methanol and biomass-derived synthetic natural gas (Searle and Malins 2015). China is an agricultural powerhouse, with a cultivation area of 114.7 million hectares for crops such as wheat, corn, soybeans, and rice. The surplus crop yield annually presents significant potential for the development of biomass energy in China (Yin *et al.* 2018).

The camphor tree, prevalent in southern China, is characterized by a lignin content comprising approximately 40% of its leaf biomass and a cellulose content of roughly 20% (MA et al. 2015). During the biomass formation process, lignin-rich substances undergo softening and melting, exhibiting adhesive properties crucial for biomass pelletization (Kaliyan and Morey 2010). Meanwhile, bamboo stands out for its exceptional carbon sequestration abilities, surpassing tree species (Wang et al. 2014). Studies reveal that bamboo forests sequester carbon at a higher rate per unit area compared to coniferous and broadleaf forests. Specifically, newly established moso bamboo forests rapidly sequester carbon during their initial three years, followed by a decrease in annual sequestration rates (Zhang et al. 2014). Furthermore, over a 60-year growth cycle, moso bamboo plantations store 1.2 times more carbon than Chinese fir plantations. In tropical settings, 10-year-old rattan bamboo plantations exhibit a carbon storage capacity 1.1 times that of tropical hardwood forests (Lou et al. 2010). The short growth cycle, robust carbon sequestration capabilities, and high economic value of bamboo are reflected in the vast bamboo forests of Zhejiang Province, covering $70.71 \times 104 \text{ hm}^2$ and sequestering 95.41 (Tg C) (Li et al. 2015). These abundant resources position bamboo as a promising reservoir for renewable energy.

Biomass energy production currently faces challenges related to the low density and high moisture content of agricultural and forestry waste. Low density leads to increased transportation and storage costs due to larger volumes. An optimal moisture level can facilitate the biomass pellet forming process by acting as both a binder and a lubricant, thereby enhancing compaction and bulk density (Shen et al. 2012; Cao et al. 2015; Kpalo et al. 2020). Removing excess moisture through heating increases the carbon content of the biomass (Pradhan et al. 2018). Densification, particularly through pelletization, is a viable solution to address these issues. Pelletization not only reduces volume but also enhances the energy content of the biomass (Bajwa et al. 2018; Iftikhar et al. 2019). This process involves extruding biomass feedstock through circular openings in a mold to produce cylindrical pellets. Effective densification requires high temperature and pressure, typically within the temperature range of 80 to 200 °C, which can significantly enhance the performance of particles (San Miguel et al. 2022). Research indicates that smaller pellets sizes during grinding lead to higher pellet densities, highlighting the direct influence of pellets size on densification (Carone et al. 2011). Furthermore, heating during the extrusion process softens the lignin within the biomass, transforming it into a natural binder (Razuan et al. 2011; Kumar et al. 2017). For optimal binding and mechanical properties, the lignin must be softened within a specific temperature range, typically between 80 to 150 °C (Samuelsson et al. 2012; Shang et al. 2012).

Biomass pellets, derived from residues and waste generated in forestry and agricultural activities, offer a renewable energy source (Xiao *et al.* 2015). In the northern region of Zhejiang Province, camphor trees, commonly used as ornamental plants, produce a copious amount of leaves annually (Ma *et al.* 2019). These leaves, rich in lignin, could serve as a natural binder in the production of biomass pellets (Kaliyan and Morey 2010). Meanwhile, in Anji County of the same province, bamboo resources often go unutilized due to various socioeconomic factors (Li *et al.* 2023). This study explores the utilization of natural materials as modifiers, with the primary objective of significantly enhancing the quality of bamboo fiber-based biomass pellets. The developed pellets exhibit notable improvements in both density and mechanical durability, thereby elevating their overall value. These advancements hold profound significance in mitigating environmental

burdens and fostering sustainable societal development. The outcomes of this research provide valuable guidance for optimizing the quality of biomass pellets.

MATERIALS AND METHODS

Biomass and its Collection

Camphor trees are mainly cultivated in the Yangtze River basin and its southwestern regions, often serving as ornamental plants in the northern part of Zhejiang Province. The bamboo industry in Zhejiang Province has developed rapidly, with an annual output value reaching 15.4 billion yuan (Li *et al.* 2023), possessing extremely important development value. The camphor tree leaves and bamboo used in this study originate from Huzhou City. The selection of these materials is based on their abundance, chemical composition conducive to energy production, and potential for sustainable utilization as biomass fuel pellets.

The main compositional parameters of the biomass materials used in the experiment are shown in Fig. 1 (Dorez *et al.* 2014; Ma *et al.* 2015). Among them, bamboo fiber has a relatively high cellulose content of approximately 58%, with a lignin content of about 20%. In contrast, camphor tree leaves have a cellulose content of approximately 20% and a lignin content of about 40%. During the hot-pressing process of pellet formation, lignin becomes softened and viscous, effectively serving as a binder. Because of the lower lignin content in bamboo fiber, adding an appropriate amount of camphor tree leaf powder with higher lignin content is expected to be beneficial for pellet formation.

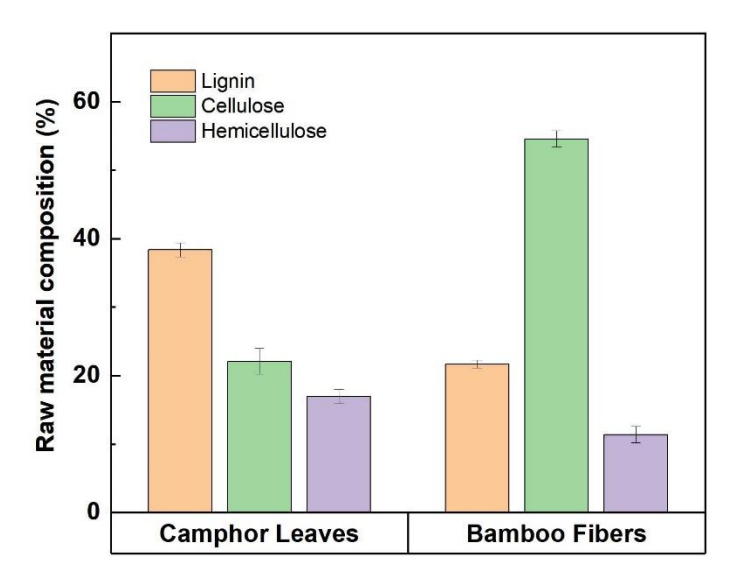


Fig. 1. Comparison of the main components of two biomass materials

Crushing and Screening of Biomass Raw Materials

Camphor tree leaves naturally fall from April to May each year. They were first swept and collected manually, and then dried in the sun for 15 days. The dried leaves were crushed using a universal pulverizer with the specified parameters in Table 1. They were processed into fiber form in a processing center (see Table 1 for processing parameters). The universal pulverizer further converted the fibrous moso bamboo into fine powder. The material was passed through a standard 0.6-mm sieve to get raw material of 0 to 0.6 mm.

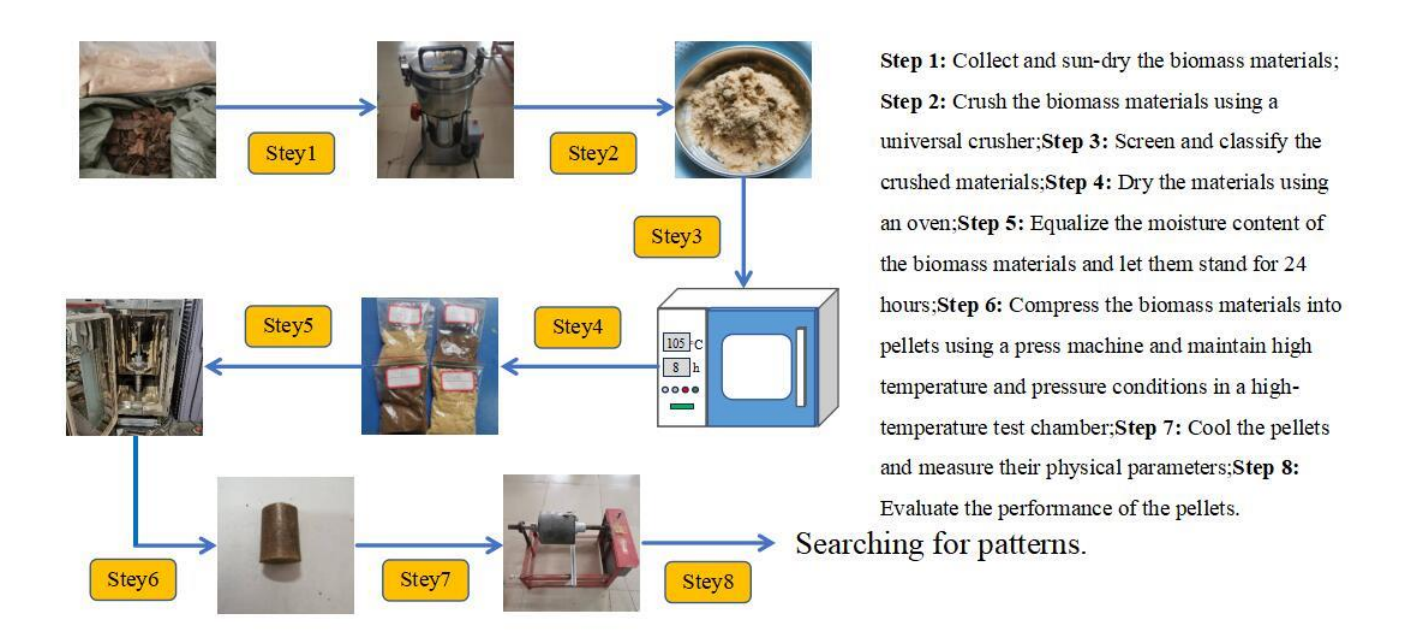
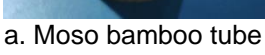


Fig. 2. Experimental flowchart for the Preparation of Biomass Pellets

 Table 1. Universal Pulverizer and Processing Center Parameters

Universal Pulverizer Specification	Measurement Unit	Parameters
Electric motor supply voltage	V	220
Electric motor rated power	W	1400
Maximum capacity	g	800
Degree of pulverization	mm	0.05
Motor speed	r/min	34000
Operating time	min	5
Processing center	Measurement unit	Parameters
specification		
Spindle speed	RPM	S5000
Feed rate	mm/min	F2000
Cutting speed	m/s	RV0.05
Per-tooth cutting depth	mm	DP10
Tool diameter	mm	D6
Number of cutting depth levels	mm	Z2







b. Processing



c. Bamboo filaments



d. Camphor leaves

Fig. 3. Raw materials

Drying of Biomass Raw Materials

The crushed biomass feedstock is dried in an oven at 105 °C for 8 h. The feedstock is then removed and weighed, with the weight recorded as m_1 . Afterwards, the material is placed back into the oven and dried at the same temperature for another 2 h. It is removed again, weighed, and the weight is recorded as m_2 . Upon removal from the oven, the moisture content of the feedstock is measured using a rapid moisture analyzer. If the weight difference between m_1 and m_2 is less than 0.5%, it is inferred that the feedstock has achieved the desired dryness and is stored in a sealed bag.

The biomass feedstock, enclosed in a sealed bag, was initially weighed and its mass recorded as m_a (g). Controlled amounts of water were then added dropwise into the sealed bag using a rubber dropper. After allowing the material to equilibrate for 24 h, it was reweighed, and the new mass was recorded as m_b (g). The moisture content (MC) of each sample was calculated using Eq. 1,

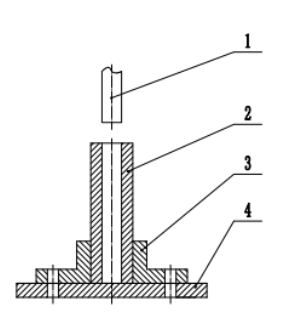
$$MC = (m_b - m_a)/(m_b - (m_a - m_2)) \times 100\%$$
 (1)

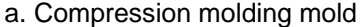
where MC is the moisture content (%), m_2 is the mass of the biomass feedstock (g), m_a is the combined mass of the biomass feedstock and the sealing bag (g), and m_b is the total mass of the biomass material along with the sealing bag after the addition of water droplets (g).

In this study, the moisture content of biomass pellets was maintained within the range of 3% to 18%. This range was chosen based on previous research (Guan *et al.* 2022) to ensure optimal combustion performance of the pellets. Studying the performance of the pellets under different conditions can provide valuable insights into their suitability for various applications and storage environments.

Forming Method

The briquetting equipment consisted of a Wance TSE105D microcomputer-controlled electronic universal testing machine (Shenzhen Wance Testing Machine Co., Ltd., Shenzhen, China), a high-temperature test chamber, and a custom-designed test mold (Fig. 4). The Wance TSE105D testing machine boasted a maximum load capacity of 100 kN with a force control rate relative error of \pm 1%. The high-temperature test chamber was equipped with PID self-stabilizing adjustment, ensuring a control accuracy of 1%.





1. Piston rod; 2. Feed sleeve;

3. Fixed support; 4. Base Mold without air vents

Fig. 4. Experimental equipment



b. Press machine



c. High temperature test

Moisture content was precisely determined using a DHS-16A moisture analyzer (Lichen Technology, Ningbo, China), offering a moisture readability down to 0.01%. Mass measurements were carried out using a high-precision Wantai electronic balance, accurate to 0.01 g. As illustrated in Fig. 4, the head of piston rod 1 was connected to the universal testing machine, which incorporated a pressure sensor. To prevent jamming between the sleeve and piston rod due to thermal expansion during the mold heating process, a carefully calculated gap was maintained between the piston rod and the feed sleeve.

Parameter Selection

In this study, with the raw material diameter (0 to 0.6 mm) and temperature (130 °C) remaining constant, the moisture content values were set at 3%, 6%, 9%, 12%, 15%, and 18% to cover the central and peripheral points of the optimal range. Pressure values of 22, 44, and 66 MPa were selected (obtained by applying forces of 5 KN, 10 KN, and 15 KN, respectively, to the compression molding die using a piston rod), along with mixing ratios of camphor tree leaves to moso bamboo fibers of 25%, 50%, 75%, and 100%, to explore various conditions. The particles used in the experiment are listed in Table 2.

 Table 2. Granular Biomass Mixture Employed for Experimentation

Composition	Abbreviation	
Moso Bamboo Fiber 100%	MB100	
Camphor Leaf 100%	CL100	
Camphor Leaf 75% Moso Bamboo Fiber 25%	CL75MB25	
Camphor Leaf 50% Moso Bamboo Fiber 50%	CL50MB50	
Camphor Leaf 25% Moso Bamboo Fiber 75%	CL25MB75	

Forming Process

The experimental process is as follows: Placed 8 g of raw material into the cavity of the compression mold. The piston rod began to move downward at a constant speed of 50 mm/min. During the movement, the particles in the compression cavity were squeezed, causing the working pressure to gradually increase. Once the working pressure reached the preset value indicated on the electronic universal testing machine, the movement of the piston rod stopped, and it entered the pressure-holding mode for 260 s for compression molding. The particles were then removed from the cavity, cooled, and stored in a sealed plastic bag.

The densification process of biomass pellets undergoes three stages (Sarker *et al.* 2023). Firstly, there is pellet rearrangement: during the initial stage, the application of compressive force causes the originally loosely arranged biomass pellets to reorganize, forming a denser structure. Gaps between pellets decrease, and the space around large pellets is filled by smaller pellets, resulting in immobile pellets. Secondly, there is plastic and elastic deformation of biomass pellets: with increasing pressure, pellets begin to compress each other, undergoing plastic and elastic deformation, thereby increasing the contact area between pellets. Large pellets may fracture into smaller ones, and electrostatic and van der Waals forces are activated to bond pellets together. Finally, there is mechanical locking between pellets: as densification progresses, mechanical locking forms between pellets, preventing deformed and fractured pellets from moving. This locking can be achieved through the formation of "solid bridges", which result from chemical reactions, sintering, hardening of binders or natural binding agents, lignin, protein compounds, and other substances formed during the densification process.

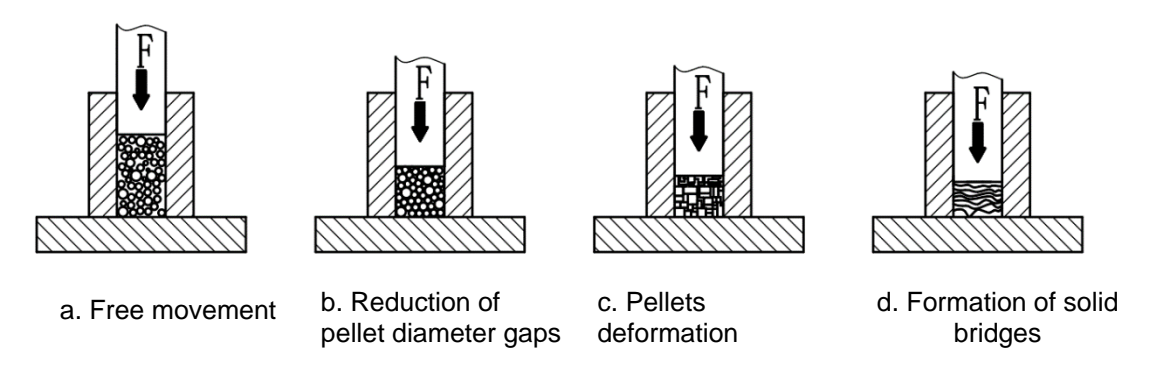


Fig. 5. The densification process of biomass pellets

Through compression and deformation, biomass pellets experience a reduction in void spaces, resulting in a significant increase in density. The mechanical locking between pellets ensures relative stability in their positions. These stages collectively contribute to the formation of a sturdy and compact structure during the densification process of biomass pellets, aiding in enhancing the stability and density of biomass materials.

Experimental Indicators

The primary experimental indicators selected for this study were pellet density (ρ) and mechanical durability (DU). The forming quality of biomass pellet fuels is paramount, with density and mechanical durability being pivotal determinants (Samuelsson *et al.* 2012). Specifically, pellet density plays a critical role in influencing energy storage efficiency, transportation feasibility, production costs, and, most importantly, combustion capacity. High-density pellets offer extended burning durations, thereby enhancing the overall utilization efficiency of biomass fuels (Miao *et al.* 2011). Therefore, it is necessary to study the molding density and molding efficiency of biomass fuel and determine the optimal combination of key factors.

Density and Mechanical Durability Testing

The length and diameter of the formed fuel pellets were recorded, and their masses were measured. The forming density was then calculated using formula Eq. 2, as outlined in the NY/T 1881.7 (2010) standard. To ensure accuracy, the final result was determined by taking the average of the densities obtained from three separate measurements,

$$\rho = 4m/(\pi d^2 h) \times 10^6 \tag{2}$$

where ρ represents the fuel density (in g/cm³), m represents the mass of each fuel piece (in g), d represents the diameter of the fuel (in mm), and h represents the length of the fuel pellet (in mm).

Mechanical durability was assessed utilizing a custom-designed rotating drum, depicted in Fig. 6. This drum was crafted in compliance with the Agricultural Industry Standard of the People's Republic of China NY/T1881 (2010), specifically the "Densified biofuel-Test methods Part 8: Mechanical durability." Its structure comprised a drum body, supports, and a cover, with all supporting elements firmly fastened by rivets.

During the mechanical durability test, the rotating drum was positioned horizontally on a rotational device, and the sample under examination was placed within

the drum. To simulate vibrations and impacts encountered during transportation, the drum was rotated at a constant speed of 40 revolutions per minute for a total of 500 revolutions.

Following this procedure, the tested sample was transferred to a circular test sieve with a pore diameter of 2.5 mm for screening, ensuring adequate separation of the pellets. Subsequently, the weight of the sample retained on the sieve was precisely measured to derive the mechanical durability data of the sample.

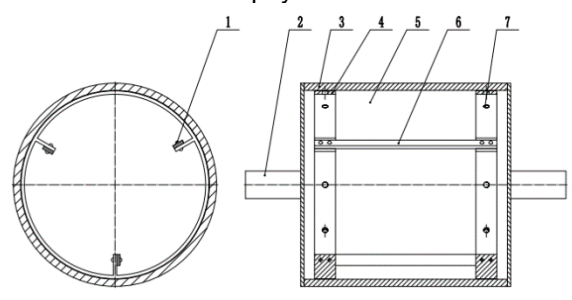
The mechanical durability of the single sample was then computed using Eq. 3 as outlined in the NY/T 1881.8 (2010) standard,

$$DU=m_A/m_E \times 100 \tag{3}$$

where DU represents mechanical durability (%), m_E represents the unscreened sample mass before drum treatment (g), and m_A represents the screened sample mass after drum treatment (g).



a. Machine physical illustration



b. Schematic diagram of the internal structure of the drum
1 Rivet; 2. Rotary shaft; 3. Outer ring; 4. Inner ring; 5. Annular chamber;
6. Iron bar; 7. Grinding hole

Fig. 6. The self-made drum and its corresponding internal structure diagram

Single-factor Experimental Design

To investigate the effects of different factors on the quality of bamboo fiber biomass granulation, sample data was collected for statistical analysis. The moisture content was set at 3%, 6%, 9%, 12%, 15%, and 18%; the molding pressure was set at 22, 44, and 66 MPa; and the proportion of moso bamboo fibers in the mixture was set at 25%, 50%, 75%, and 100%. Each experiment was repeated three times. The density of the obtained particles was calculated using Eq. 2, and the influence of these three factors on density was analyzed. The mechanical durability was tested using the machine shown in Fig. 6, and the mass of the particles before and after testing was recorded. Equation 3 was used to determine mechanical durability, and the impact of these three factors on this metric was analyzed.

RESULTS AND DISCUSSION

Imaging Results of the Cross-Section of Biomass Pellets

Two biomass pellet types, MB100 and CL50MB50, produced under the same conditions, were selected for comparison. Scanning electron microscopy (S-3400N; Hitachi Ltd, Tokyo, Japan) was used to observe the cross-sections of the samples, and the results are illustrated in Figs. 7a and 7b. In the cross-section of MB100, the pure bamboo fiber pellets exhibit a "vermicular" or "worm-like" appearance with fewer stable "solid bridges' structures. This morphology resulted in a significantly lower pellet density compared to that of CL50MB50. In contrast, the mixed pellets of CL50MB50 reveal a "shale-like" structure where leaf vein vascular bundles and fine wood fibers are intertwined. This leads to more compact pellets with fewer pores. Under high temperature and pressure conditions, the "solid bridges" become stronger and more structurally stable. The microscopic differences between these two pellet types are attributed to the higher proportion of lignin in camphor tree leaves. Lignin, which can act as a natural adhesive during the hot-pressing process, contributes to forming stronger and more durable pellets.

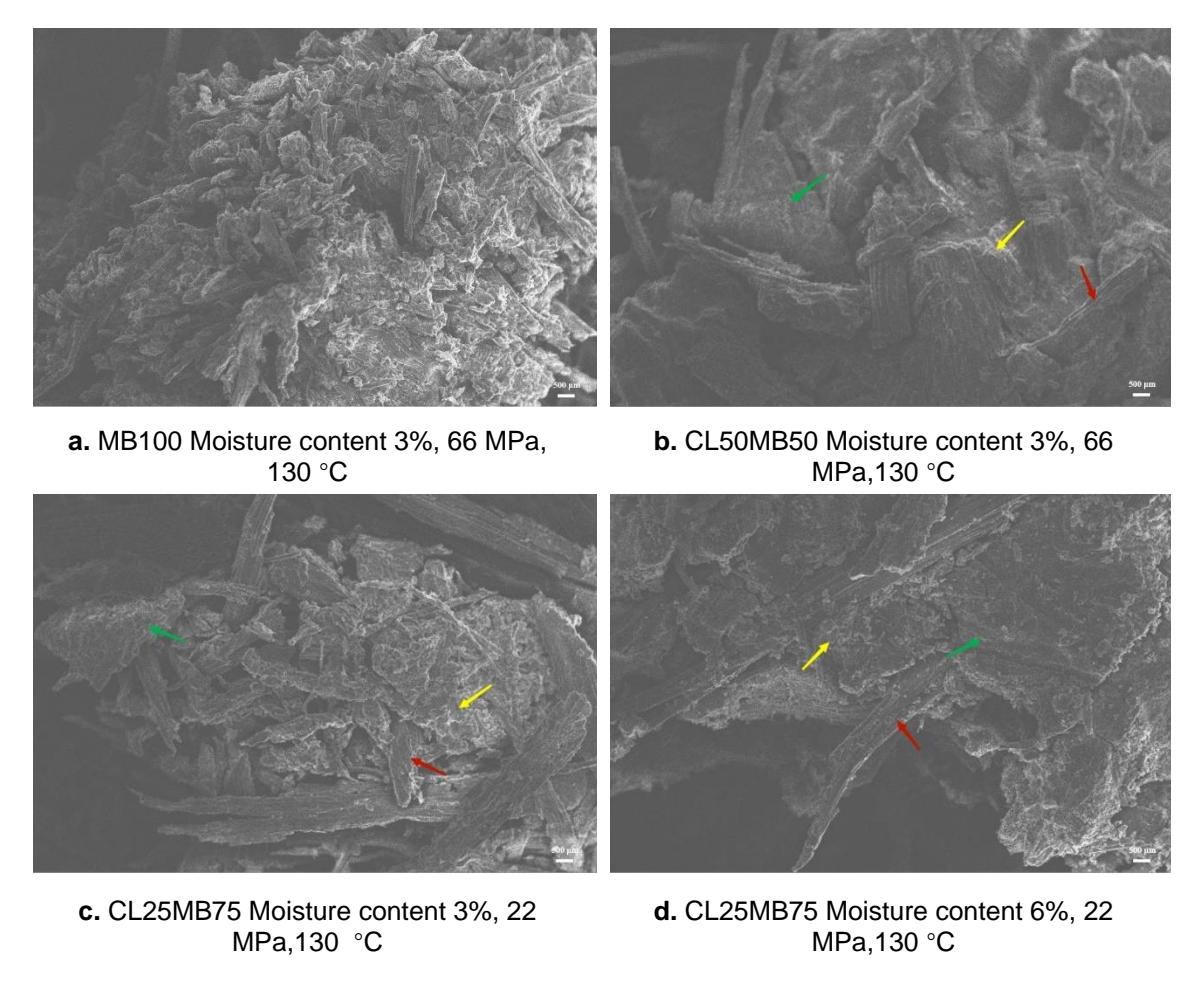


Fig. 7. SEM images: the red arrow indicates bamboo fibers, the yellow arrow indicates camphor leaf powder, and the green arrow indicates the "solid bridge"

Figures 7c and 7d illustrate that as the moisture content of CL25MB75 slightly increased from 3% to 6%, the connecting "solid bridges" between particles exhibited a

smoother texture, with reduced tearing and a polished pellet surface. Consequently, this led to an elevation in pellet density. This phenomenon is hypothesized to be influenced by the enhanced lignin softening efficiency due to the increased moisture content during the pellet formation process. In the pellets, the leaf vein vascular bundles of camphor leaves intertwined with fine lignocellulosic fibers, and lignin softens during the molding process to function as a natural binder. The formation of "X" structures led to a more densely packed and intricate interconnection within the pellet interior, resulting in an increase in pellet density. This compact internal structure enhances the mechanical durability of the pellets, enabling them to maintain their integrity during loading, unloading, conveying, and transportation processes.

The Impact of Moisture Content on the Surface of Formed Pellets

Observations of particle surface characteristics reveal significant differences under various moisture content conditions. Taking CL25MB75 (Fig. 8) as an example, particles with a 3% moisture content exhibited cracks on their surface. However, within the moisture content range of 6% to 9%, the particles demonstrated optimal forming effects and surface quality, with almost no visible cracks. At a 12% moisture content, the particles showed good forming effects and surface quality, with only minor cracks visible on the dense and solid fuel particles. When the moisture content reached 15%, a pronounced popping or "explosion" phenomenon occurred, resulting in a rough particle surface, increased cracks, and even bending of the particles. At an 18% moisture content, this explosive behavior became more severe, significantly affecting the forming effect and even causing some samples to fail to form completely.

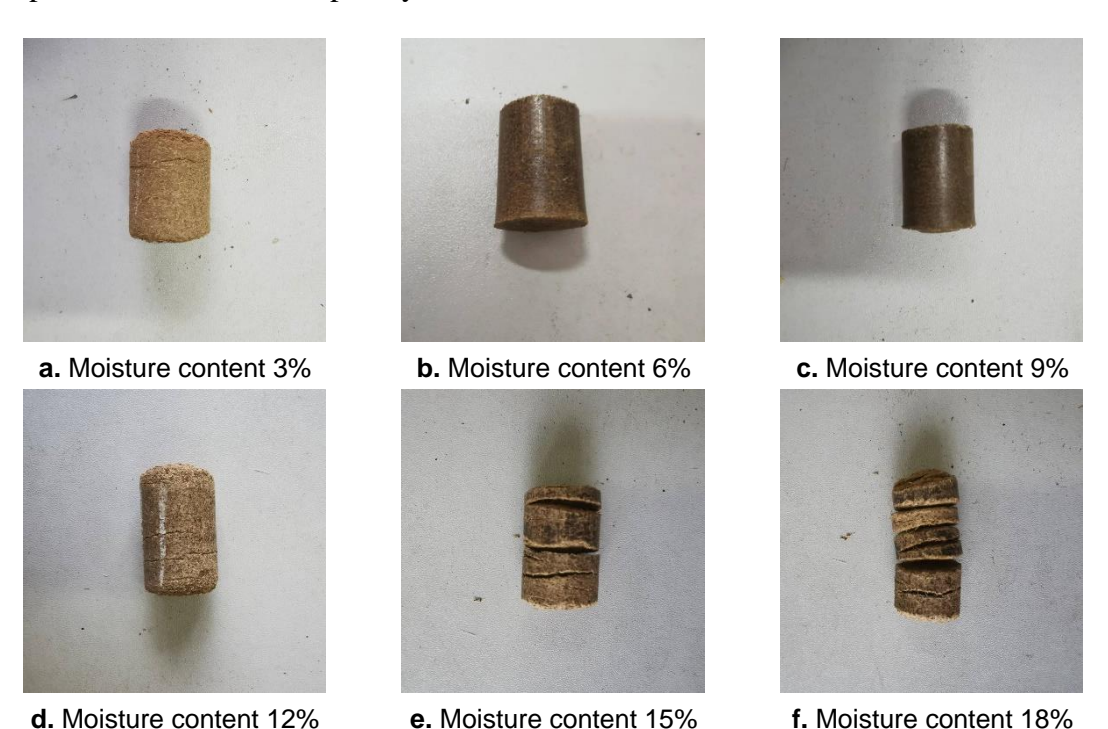


Fig. 8. Effect of different moisture contents on the surface of formed pellets (CL25MB75, 130 °C, Molding pressure 44 MPa)

The Influence of Moisture Content and Pressure on Density

The experimental results are presented in Fig. 9. In Fig. 9a, CL25MB75 achieved a density of 0.94 g/cm³ at a moisture content of 3%, which was higher than other particles. When the moisture content increased to 6%, the upward trend in density for CL25MB75 was less pronounced than for other particles, and its density was surpassed by CL50MB50. When the moisture content increased to 9%, the density of CL25MB75 was only slightly higher than MB100. In Fig. 9b, CL50MB50 maintained its advantage at moisture contents of 3% and 6%, but it was surpassed by CL75MB25 at a moisture content of 9%. In Fig. 9c, CL50MB50 maintained its superiority within the moisture content range of 3% to 9%, but it was overtaken by CL75MB25 at a moisture content of 12%. All three charts in Fig. 9 exhibit a similar pattern: the forming density of the particles performed well within the moisture content range of 3% to 9%, with an overall upward trend in density; however, within the range of 9% to 18%, the density showed an overall downward trend. At a moisture content of 12%, small damages began to appear in the raw materials, and these damages become more severe as the moisture content increased. This suggests that at a moisture content of 12%, the content of free water and bound water in the biomass particles reaches a critical point, the internal voids tend to be filled, and excess water begins to accumulate at the bottom of the particles. As the moisture content increases, large and dense cracks appear in localized positions of the particles, thereby reducing the density of the formed particles.

Under varying forming pressures and moisture contents, MB100 exhibited poor density performance. However, the addition of different proportions of camphor tree leaves improved the quality of the particles. This improvement is attributed to the high lignin content of camphor tree leaves, which enables the formation of a better "solid bridge" effect during the particle forming process. The "solid bridge" is formed by the hardening of natural adhesives, such as lignin and protein compounds, during the densification process, thereby enhancing the density of the particles.

With the increase in forming pressure, the particle density generally showed an upward trend. This result indicates that higher pressure promotes the decomposition of larger biomass particles into smaller ones, leading to deformation and plastic flow. These smaller particles more effectively fill voids, allowing for tighter contact and interlocking between them. This process ultimately contributes to the overall improvement in the bulk density of biomass particles.

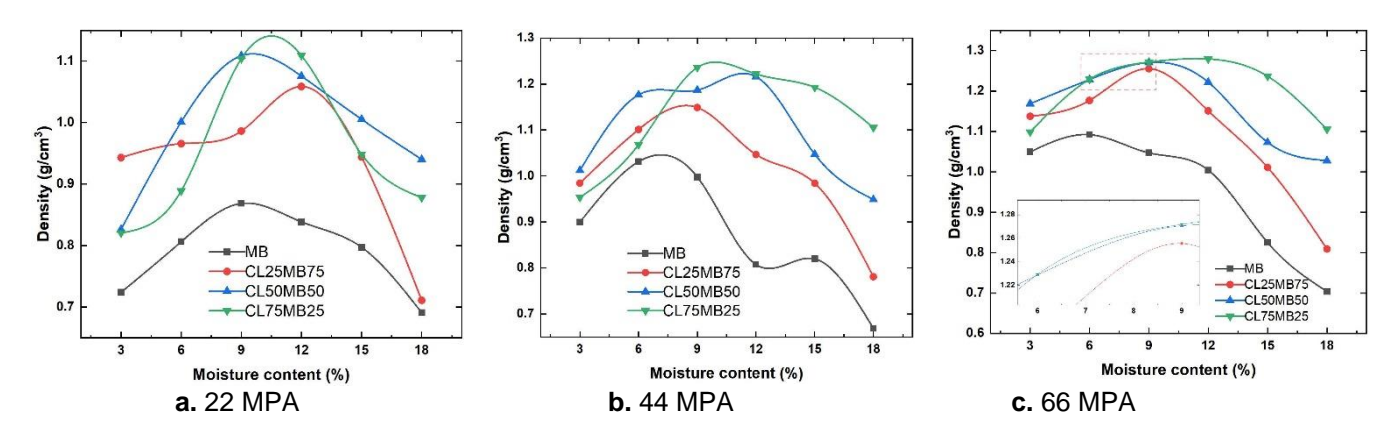


Fig. 9. The relationship between moisture content and density changes

Analysis of the Increasing Range of Pellet Density

Based on the increasing range of pellet density from 3 to 9% shown in Fig. 9, Fig. 10 was then plotted. From Fig. 10, the impact of moisture content and molding pressure on density can be more intuitively perceived. With the increase in molding pressure, the density of all pellets increased accordingly. Except for the MB100 sample, the density patterns of the other samples indicate that as the moisture content rose from 3% to 9% under different molding pressures, the pellets became more compacted.

As the content of camphor tree leaves increased from 0% to 25%, the pellet density increased significantly, with a maximum increase of 23%. When the camphor tree leaf content was increased from 25% to 50%, the pellet density continued to rise, but the increase was less significant, with a maximum increase of 11%. As the camphor tree leaf content further increased to 75%, the maximum density increase was 4%. This suggests that adding an appropriate amount of camphor tree leaf powder can facilitate pellet formation. The optimal amount to be added will be determined through subsequent orthogonal experiments.

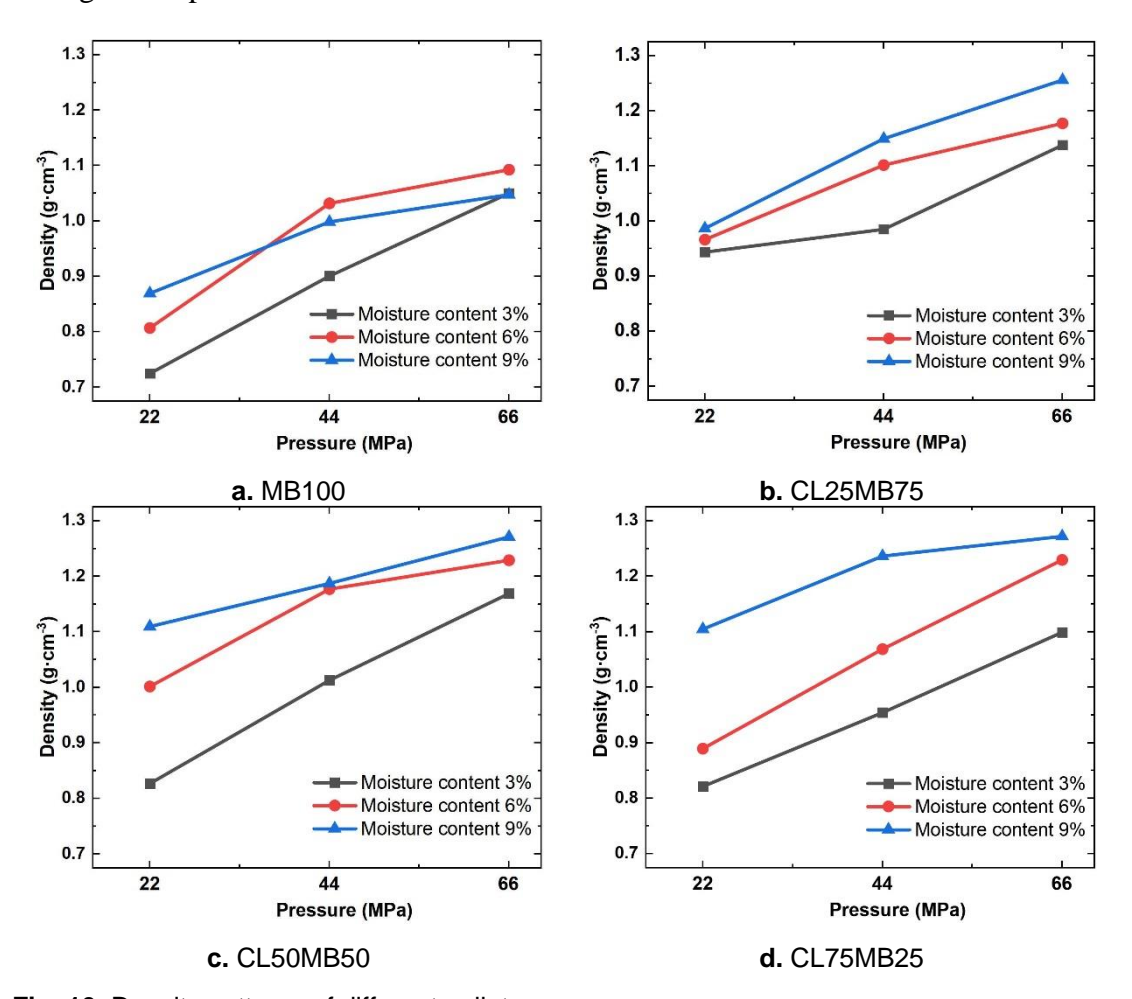


Fig. 10. Density patterns of different pellets

Influence of Moisture Content and Pressure on Mechanical Durability

The experimental results are shown in Fig. 11. In Fig. 11a, as the moisture content increased from 3% to 9%, the mechanical durability of the pellets improved. However, as the moisture content increased from 9% to 18%, the mechanical durability rapidly

decreased. Within the moisture content range of 6% to 12%, the mixed pellet samples exhibited over 90% mechanical durability under different forming pressures. At a moisture content of 3% and a forming pressure of 22 MPa, the durability of most samples was below 90%, except for the CL50MB50 sample. In Fig. 11b, the mechanical durability of MB100 with a moisture content of 3% was below 85%. When the forming pressure was increased to 44 MPa, its mechanical durability exceeded 90%. In Fig. 11c, when the forming pressure was increased to 66 MPa, all pellets exhibited mechanical durability greater than 90% within the moisture content range of 3% to 12%, followed by a decline. Except for CL50MB50 with a moisture content of 3% in Fig. 11b, pure bamboo fibers performed poorly compared to pellets mixed with camphor tree leaves due to their lack of a stable structure formed by the camphor tree leaf's vein vascular bundles and the fine woody fibers interspersed within them, resulting in poor performance in most tests.

The trend of mechanical durability typically increases first and then decreases with an increase in moisture content. When the forming pressure remains constant, mechanical durability often shows an upward trend as the moisture content ranges from 3% to 9%. However, when the moisture content was further increased from 9% to 18%, the mechanical durability initially remained stable and then began to decline. When the forming pressure was increased, the mechanical durability of pellets with a 3% moisture content rapidly improved. This suggests that when the pressure is too low, the free water and bound water in the raw material cannot fully fill the internal voids, thus failing to function as a natural adhesive. Consequently, during mechanical durability testing, the formed pellets cannot effectively resist the impacts simulated during drops and transportation.

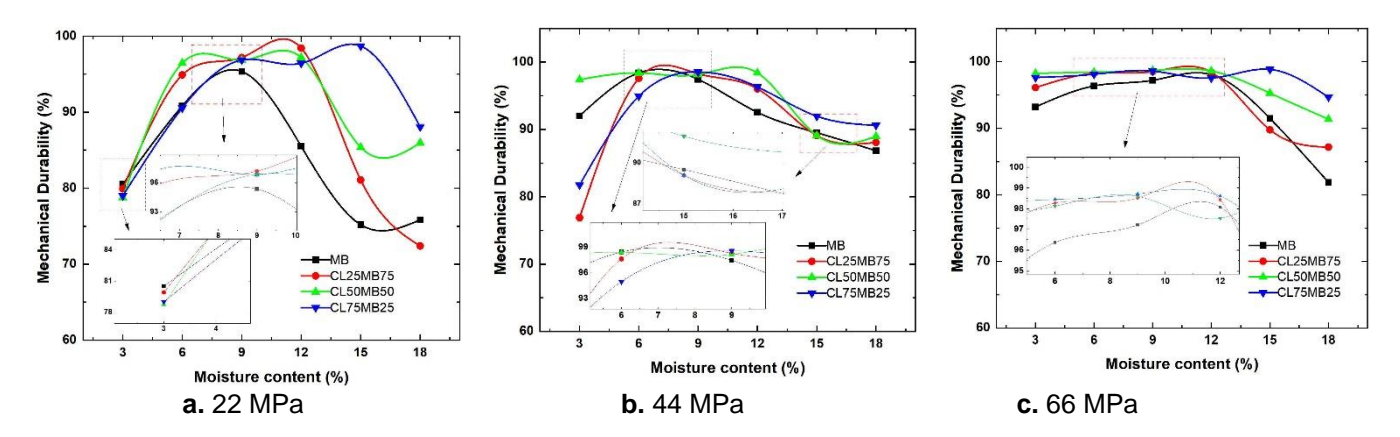


Fig. 11. The relationship between mechanical durability and density change

Three-dimensional Curved Surface Plots of Different Pellets

Through the analysis of the three-dimensional surface graph shown in Fig. 12, it becomes evident that as both moisture content and forming pressure gradually increased, the mechanical durability of the pellets exhibited a trend that was remarkably similar to the variation in density. Based on this observation, it is inferred that a strong correlation between the density of the pellets and their mechanical durability exists. This correlation suggests that an increase in pellet density can directly influence its mechanical durability, thereby enhancing the pellets' resistance to drops and impacts during transportation.

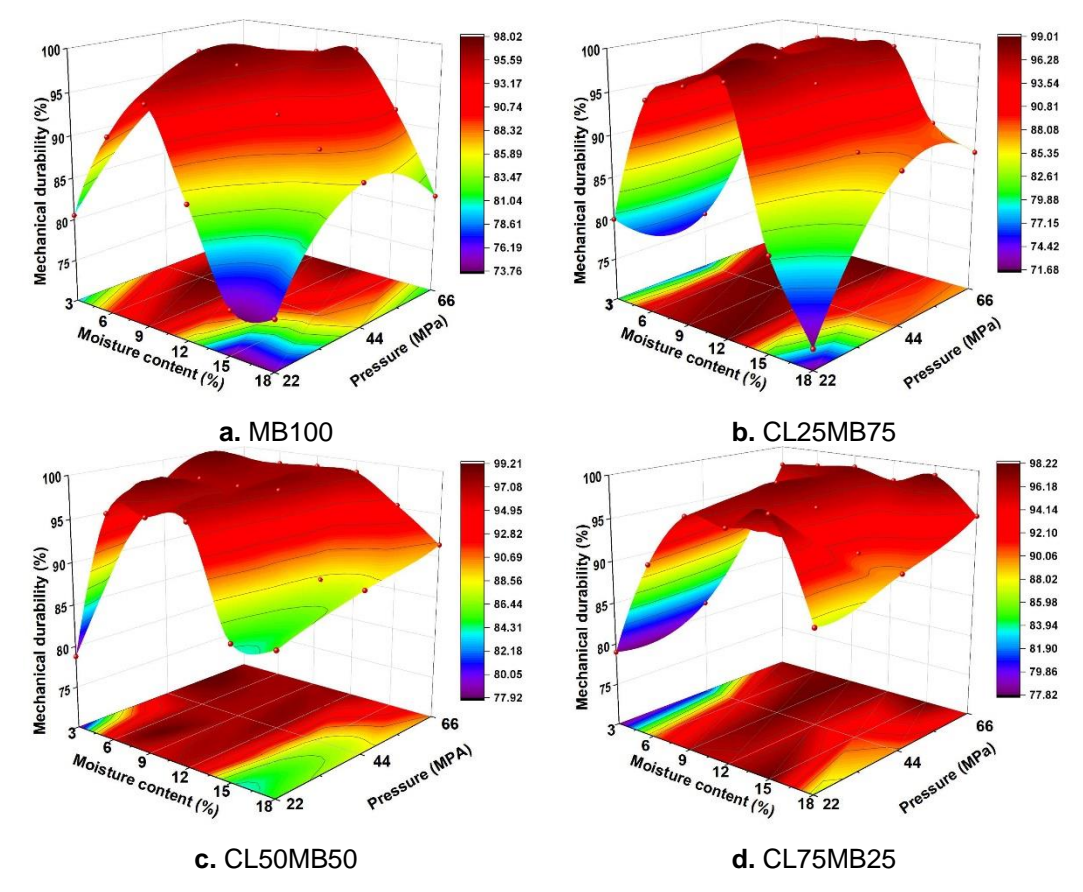


Fig. 12. Three-dimensional curved surface graph of the influence of moisture content and pressure on mechanical durability

Correlation of Density with Mechanical Durability

Based on the density and mechanical durability data collected from all samples, a linear fitting curve was plotted, as shown in Fig. 13. The figure clearly demonstrates that as density was gradually increased, there was a corresponding improvement in mechanical durability. Equation 4 can be used to calculate the density required for pellets to achieve high mechanical durability.

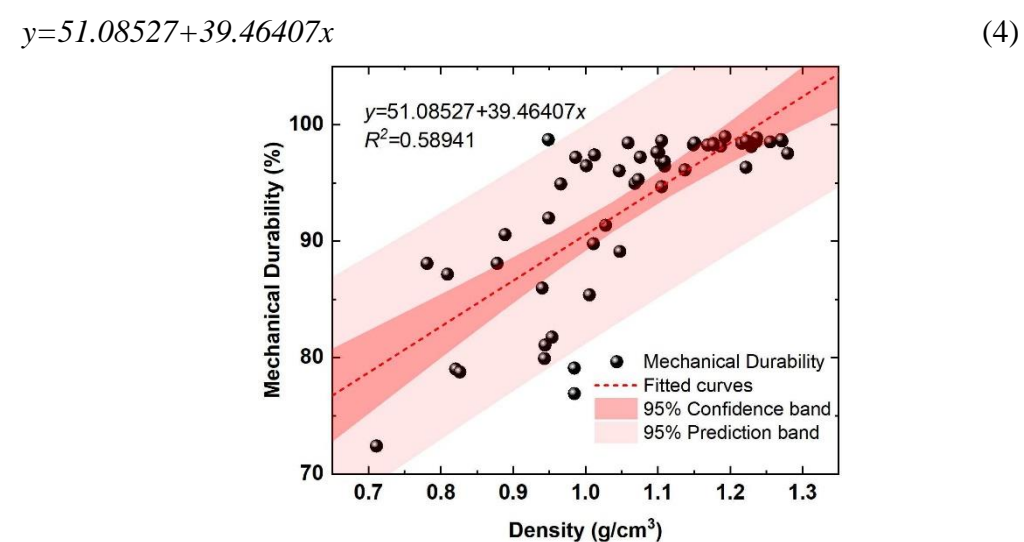


Fig. 13. Density and mechanical durability correlation curve

Based on Fig. 13, it can be concluded that to achieve a mechanical durability of 90%, the density of the compacted sample should exceed $0.986~g/cm^3$. To obtain a mechanical durability of 95%, the density of the compacted sample should surpass $1.1128~g/cm^3$.

Orthogonal Experimental Design and Result Analysis

Based on the aforementioned experimental results, both density and mechanical durability exhibited relatively high values within the moisture content range of 3% to 9%. To further explore the impact of various parameters on these two key indicators and determine the optimal conditions for producing biomass pellets, the authors conducted an orthogonal experimental design. Density and mechanical durability were selected as the primary evaluation metrics and the following parameters focused on moisture content (A), mixing ratio of camphor tree leaves (B), and forming pressure (C).

Table 3. Orthogonal Test Results

No.	Factors and Interaction Factors		Test Results					
	Α	В	Blank	С	Density ρ 1/(g·cm³)	Density ρ 1/(g·cm³)	Mechanical Durability (DU1/%)	Mechanical Durability (DU2/%)
1	1	1	1	1	0.801	0.827	80.367	82.990
2	1	2	3	2	0.911	0.986	88.123	92.253
3	1	3	2	3	1.064	1.087	93.160	93.130
4	2	1	3	3	1.139	1.226	97.873	98.680
5	2	2	2	1	0.912	0.953	91.000	90.103
6	2	3	1	2	1.054	1.094	96.517	96.573
7	3	1	2	3	1.137	1.239	98.043	98.170
8	3	2	1	2	1.022	1.157	95.890	98.163
9	3	3	3	1	0.977	1.031	93.537	95.443

Note: A is moisture content, B is particle size, C is forming pressure

Table 4. Analysis of Extreme Differences

Indicators	Parameters	Factors			
		Α	В	Blank	С
	<i>K</i> ₁	5.676	6.369	5.955	5.955
	K ₂	6.381	5.941	6.392	6.392
	<i>K</i> ₃	6.563	6.307	6.270	6.892
Doneity	<i>k</i> 1	0.946	1.062	0.993	0.993
Density	<i>k</i> ₂	1.064	0.990	1.065	1.065
	k 3	1.094	1.051	1.045	1.149
	R	0.148	0.071	0.073	0.156
	Rank	2	4	3	1
	K ₁	530.023	556.123	550.500	533.440
	K ₂	570.746	555.532	563.606	567.519
	<i>K</i> ₃	579.246	568.360	565.909	579.056
Machanical durability	<i>k</i> 1	88.337	92.687	91.750	88.907
Mechanical durability	k ₂	95.124	92.589	93.934	94.587
	k 3	96.541	94.727	94.318	96.509
	R	8.204	2.138	2.568	7.603
	Rank	1	4	3	2

Note: K is the sum of the cells that meet the requirements; k is the arithmetic mean value of K; R is range

Each factor was set at three levels: moisture content at 3%, 6%, and 9%; the proportion of camphor tree leaves added to the pellets at 25%, 50%, and 75%; and forming pressure at 22, 44, and 66 MPa. Each combination of factors was repeated twice, and each group was replicated three times. The results are presented in Table 3.

Table 5. Analysis of Variance

Indexes	Source	Sum of Squares	Mean Square	F value	Significance
	Α	230.751	115.375	49.096	< 0.001**
Mechanical durability	В	25.014	12.507	5.322	0.024*
iviechanical durability	С	195.05	97.525	41.5	< 0.001**
	Error	25.85	2.35		
	Α	0.073	0.036	15.528	0.001*
Density	В	0.003	0.001	0.556	0.589
Density	С	0.146	0.073	31.083	< 0.001**
	Error	0.026	0.002		

Note: *Indicates that the difference was significant (P < 0.05); ** Indicates that the difference was extremely significant (P < 0.01)

When analyzing the factors that affect the density of biomass pellets, it can be observed from Table 5 that both moisture content and forming pressure were statistically significant (P < 0.05), indicating a differential relationship between these factors and this key indicator. From Table 4, it is evident that the hierarchical order of influence on bulk density during the formation of biomass pellets was C > A > B. This suggests that forming pressure (C) was the most influential factor on density, followed by moisture content (A). In comparison, the mixing ratio (B) had a relatively minor impact. Therefore, the optimal parameter combination was determined to be $A_3B_1C_3$, which corresponds to a moisture content of 9%, a forming pressure of 66.085 MPa, and a mixing ratio of CL25MB75.

When exploring the factors that affect mechanical durability, Table 5 reveals that moisture content, mixing ratio, and forming pressure were all statistically significant (P < 0.05). This implies that these factors had varying degrees of impact on the mechanical durability of the pellets. According to the ranking in Table 4, the order of influence was A > C > B. Moisture content (A) emerged as the most critical determinant of mechanical durability, followed by forming pressure (C), and finally, mixing ratio (B). Consequently, the optimal parameter combination was identified as $A_3B_3C_3$, which corresponds to a moisture content of 9%, a forming pressure of 66.085 MPa, and a mixing ratio of CL75MB25.

Superior Sample Analysis

The stress relaxation behavior of compressed biomass pellet samples, specifically CL25MB75 and CL75MB25, is illustrated in Fig. 14. These curves depict how the stress in the samples gradually decreased over time when subjected to an initial compressive load. It is noteworthy that the shape of these stress relaxation curves was influenced by the magnitude of the initially applied compressive load. Higher maximum loads during compression resulted in greater residual stress within the samples (Johnson *et al.* 2013). This residual stress can be quantitatively assessed using Eq. 5, which provides a mathematical representation of the stress relaxation phenomenon observed in the experiments,

$$Y(t) = (\sigma_0 - \sigma_t)/\sigma_0 \times 100\% \tag{5}$$

where Y(t) is a parameter showing the decay of the stress as a function of time t (%), σ_0 is initial stress (MPa), and σ_t is stress at time t (MPa).

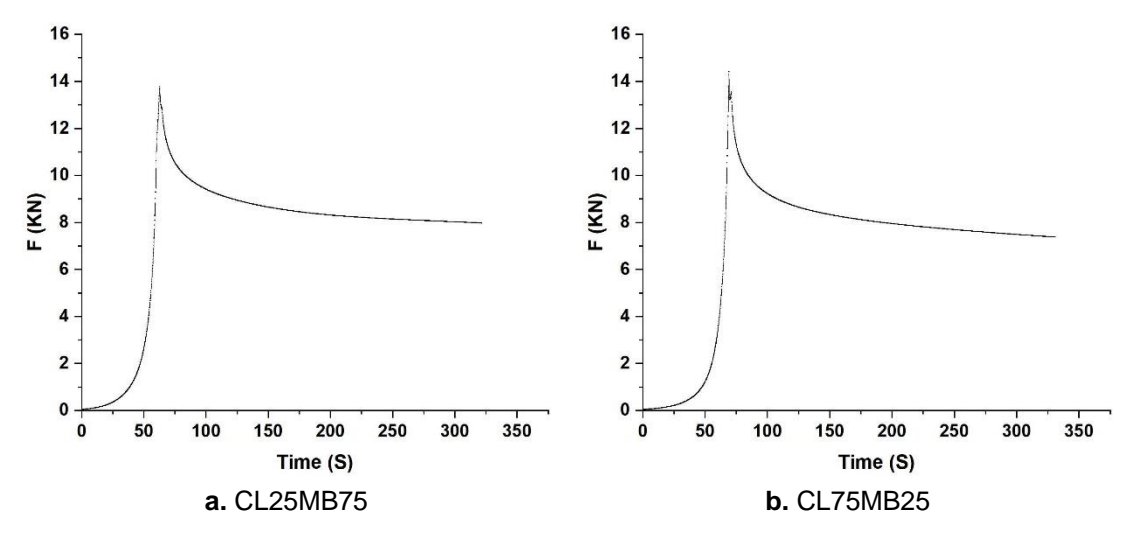


Fig. 14. Stress relaxation and time curve

The stress relaxation rate is a key parameter that quantifies the ratio between the amount of stress relaxed within a short time interval and the total stress relaxation observed over a longer period. This ratio serves as an indicator of the rate at which stress decays within the material during the initial stages of relaxation (Guo *et al.* 2016). To calculate the stress relaxation rate, Eq. 6 was used, which provides a specific mathematical expression for this important metric,

$$RR = (\sigma_0 - \sigma_{t1}) / (\sigma_0 - \sigma_{t=240}) \times 100\%$$
 (6)

where RR is a decay parameter (%), σ_0 is initial stress (MPa), σ_{t1} is stress at time t1 (MPa), and $\sigma_{t=240}$ is stress at time t = 240 s (MPa).

The relaxation process commenced immediately after the compression process was concluded. This process can be divided into two distinct phases. In the initial phase, the residual stress resulting from compression experienced a rapid decay within the first few minutes. Subsequently, in the second phase, the stress gradually tapered off to a stable value that varied with time. As illustrated in Table 5, the relaxation values for CL25MB75 samples ranged from 34.8% to 41.8%, while those for CL75MB25 samples spanned from 40.4% to 48.3%, both measured within a timeframe of 60 to 240 s. Once the preset pressure was attained, a notable decrease in the compression-induced residual stress was observed during the first 60 s of pressure maintenance, followed by a more gradual decline. This pattern of stress relaxation provides insights into the material's ability to retain its shape and structural integrity under compressive loads.

At $\sigma_{t1} = 60$, the RR was 83%. At $\sigma_{t1} = 90$, the RR was 88%; and at $\sigma_{t1} = 120$, the RR was 90%. The decay of stress was 83% at 60 s, indicating that as time increases, the decay rate slows down. This suggests that the pellets gradually reach a relatively stable state, leading to a reduction in the release of residual stress.

In biomass pellets, lower residual stress is more desirable. Reduced residual stress contributes to minimizing internal structural damage and interactions between pellets, thereby enhancing their mechanical stability and durability. This is beneficial in reducing pellet damage during storage, transportation, and handling, making it more advantageous

for biomass pellet applications. From a production standpoint, the pressure holding time should not be excessively long, but an overly brief pressure holding period can lead to excessive residual stress. Therefore, it is crucial to select an appropriate pressure holding time. Referring to Table 6, over 30% of stress decay in the samples occurred within 60 s. Using this as a reference, the optimal pressure holding time for large-scale production of biomass pellets made from a mixture of camphor leaves and moso bamboo was judged to be S = 60.

Table 6. Extent of Relaxation

	<i>Y</i> (<i>t</i>) %	<i>Y</i> (<i>t</i>) %	RR %	RR %
	CL25MB75	CL75MB25	CL25MB75	CL75MB25
σ_{60}	34.84	40.45	83.37	83.74
σ_{90}	37.38	42.80	89.45	88.61
σ_{120}	39.01	44.40	93.34	91.91
σ_{240}	41.79	48.30	-	-

Analysis on Heating Value of Biomass Pellets

A list of calorific values of common biomass solid fuels is provided in Table 7 for reference (Parikh *et al.* 2005). The four mixed pellets with different proportions and MB100 used in the experiment had undergone high heating value and lower heating value tests, and the results are shown in Table 8.

Table 7. Common Biomass Calorific Value

No	Raw Material	HHV (Kcal/kg)
1	Wood Chips	4832.58
2	Pistachio shell	4477.54
3	Cotton shells	3953.4
4	Corncob	4548.89
5	Bagasse	3192.08
6	Wheat straw	4308.21
7	Rice straw	3884.94

Table 8. Calorific Value of Biomass Pellets

No	Raw Material	HHV (Kcal/kg)	LHV (Kcal/kg)
1	MB100	4496.67	4435.67
2	CL25MB75	4377	4233.33
3	CL50MB50	4297	4152.33
4	CL75MB25	4321.33	4161.67
5	CL100	4545.67	4364.33

Table 8 shows that the higher heating value and lower heating value of all types of pellets were greater than 4000 Kcal/kg. The high heating value ensures their efficiency as fuel, while the lower heating value is also maintained at a relatively high level, indicating their ability to provide energy continuously and stably during the combustion process. These pellets are crafted from biomass materials, which are abundantly available and renewable, thereby promoting resource recirculation and sustainable development. This not only aligns with environmental sustainability goals but also carries significant economic value.

CONCLUSIONS

- 1. The addition of appropriate amounts of camphor tree leaf powder to bamboo fibers can effectively enhance the quality of the pellets. This is attributable to the higher lignin content in camphor tree leaves compared to bamboo fibers. Lignin can serve as a natural adhesive during the hot-pressing process. The vascular bundles of the camphor tree leaves intertwined with fine lignocellulosic fibers form a stable structure, enabling the mixed pellets to better resist vibrations and impacts during transportation.
- 2. As the moisture content of the raw material increased from 3% to 9% under constant molding pressure, the density and mechanical durability of the pellets was enhanced. Further elevating moisture to 12% initially stabilized these properties, but thereafter a rapid decline was observed. At low moisture content (3%), an increase in molding pressure significantly enhanced the density and mechanical durability of the molded fuel. There is a positive correlation between density and mechanical durability.
- 3. Based on the results of orthogonal experiments, both moisture content and molding pressure were found to have significant effects on density and mechanical durability. Under the conditions of a temperature of 130 °C, a pressure of 66.085 MPa, and a moisture content of 9%, the sample with the best molding density was obtained for CL25MB75, while the sample with the best mechanical durability was CL75MB25.
- 4. Through analyzing the stress relaxation and time curves of the CL25MB75 and CL75MB25 sample pellets, the results indicate that within 60 seconds, the pellet samples underwent over 30% stress attenuation, with a gradual slowdown thereafter. According to the calorific value test results, both the higher and lower heating values of the pellets were greater than 4000 Kcal/kg, indicating significant economic value.

ACKNOWLEDGMENTS

This research was supported by Zhejiang Provincial Natural Science Foundation of China under Grant No. LY20E080008. A Project Supported by Scientific Research Fund of Zhejiang Provincial Education Department (No.Y202353779). A Project Supported by Public Welfare Technology Applied Research in Huzhou City (Key) (2020GZ15).

REFERENCES CITED

- Bajwa, D. S., Peterson, T., Sharma, N., Shojaeiarani, J., and Bajwa, S. G. (2018). "A review of densified solid biomass for energy production," *Renewable and Sustainable Energy Reviews* 96, 296-305. DOI: 10.1016/j.rser.2018.07.040
- Cao, L., Yuan, X., Li, H., Li, C., Xiao, Z., Jiang, L., Huang, B., Xiao, Z., Chen, X., Wang, H., *et al.* (2015). "Complementary effects of torrefaction and co-pelletization: energy consumption and characteristics of pellets," *Bioresource Technology* 185, 254-262. DOI: 10.1016/j.biortech.2015.02.045
- Carone, M. T., Pantaleo, and Pellerano. (2011). "Influence of process parameters and biomass characteristics on the durability of pellets from the pruning residues of *Olea europaea* L," *Biomass and Bioenergy* 35(1), 402-410. DOI: 10.1016/j.biombioe.2010.08.052

- Dorez, G., Ferry, L., Sonnier, R., Taguet, A., and Lopez-Cuesta, J. M. (2014). "Effect of cellulose, hemicellulose and lignin contents on pyrolysis and combustion of natural fibers," *Journal of Analytical & Applied Pyrolysis* 107, 323-331. DOI: 10.1016/j.jaap.2014.03.017
- Guo, L., Wang, D., Tabil, L. G., and Wang, G. (2016). "Compression and relaxation properties of selected biomass for briquetting," *Biosystems Engineering* 148, 101-110. DOI: 10.1016/j.biosystemseng.2016.05.009
- Iftikhar, M., Asghar, A., Ramzan, N., Sajjadi, B., and Chen, W. Y. (2019). "Biomass densification: Effect of cow dung on the physicochemical properties of wheat straw and rice husk based biomass pellets," *Biomass and Bioenergy* 122, 1-16. DOI: 10.1016/j.biombioe.2019.01.005
- Johnson, P., Cenkowski, S., and Paliwal, J. (2013). "Compaction and relaxation characteristics of single compacts produced from distiller's spent grain," *Journal of Food Engineering* 116(2), 260-266. DOI: 10.1016/j.jfoodeng.2012.11.025
- Guan, X., Zhang, Y., Xu, Y., Tao, L., Hu, X., Zhou, Z., and Zhang, L. (2022). "Effects of raw material particle size and moisture content on the density and mechanical durability of camphor tree leaf pellet fuel," *Transactions of the Chinese Society of Agricultural Engineering* 14, 227-234. DOI: 10.11975/j.issn.1002-6819.2022.14.026
- Kaliyan, N., and Morey, R. V. (2010). "Natural binders and solid bridge type binding mechanisms in briquettes and pellets made from corn stover and switchgrass," *Bioresource Technology* 101(3), 1082-1090. DOI: 10.1016/j.biortech.2009.08.064
- Kpalo, S. Y., Zainuddin, M. F., Manaf, L. A., and Roslan, A. M. (2020). "A review of technical and economic aspects of biomass briquetting," *Sustainability* 12(11), article 4609. DOI: 10.3390/su12114609
- NY/T 1881-2010 (2010). "Densified biofuel-Test methods Part 8: Mechanical durability," National Standards of the People's Republic of China, Beijing, China.
- NY/T 1881-2010 (2010). "Densified biofuel-Test methods Part 7: Particle density," National Standards of the People's Republic of China, Beijing, China.
- Kumar, L., Koukoulas, A. A., Mani, S., and Satyavolu, J. (2017). "Integrating torrefaction in the wood pellet industry: a critical review," *American Chemical Society* 31, 37-54. DOI: 10.1021/acs.energyfuels.6b02803
- Li, L., Zhu, H., Wu, T., Wei, L., and Li, N. (2023). "New landscape-perspective exploration of Moso bamboo forests under on/off-year phenomena and human activities," *Frontiers in Forests and Global Change* 6, article ID 1204329. DOI: 10.3389/FFGC.2023.1204329
- Li, P., Zhou, G., Du, H., Lu, D., Mo, L., Xu, X., Shi, Y., and Zhou, Y. (2015). "Current and potential carbon stocks in Moso bamboo forests in China," *Journal of Environmental Management* 156, 89-96. DOI: 10.1016/j.jen-vman.2015.03.030
- Lin, B., and Xu, B. (2020). "How does fossil energy abundance affect China's economic growth and CO₂ emissions?," *Science of The Total Environment* 719, article ID 137503. DOI: 10.1016/j.scitotenv.2020.137503
- Lou, Y., Li, Y., Buckingham, K., Henley, G., and Zhou, G. (2010). *Bamboo and Climate Change Mitigation: A Comparative Analysis of Carbon Sequestration* (Technical Report No. 32), International Network for Bamboo and Rattan, Beijing, China.
- Ma, Y., Wang, B., Zhang, R., Gao, Y., and Zuo, Z. (2019). "Initial simulated acid rain impacts reactive oxygen species metabolism and photosynthetic abilities in *Cinnamomum camphora* undergoing high temperature," *Industrial Crops and Products* 135, 352-361. DOI: 10.1016/j.indcrop.2019.04.050

- Ma, Z., Gao, S., Yang, W., and Wu, F. (2015). "Degradation characteristics of lignin and cellulose of foliar litter at different rainy stages in subtropical evergreen broadleaved forest," *Chinese Journal of Ecology* 34(1), article 18. DOI: 10.13292/j.10004890.2015.0018
- Miao, Z., Grift, T. E., Hansen, A. C., and Ting, K. C. (2011). "Energy requirement for comminution of biomass in relation to particle physical properties," *Industrial Crops and Products* 33(2), 504-513. DOI: 10.1016/j.indcrop.2010.12.016
- Olabi, A. G., and Abdelkareem, M. A. (2022). "Renewable energy and climate change," *Renewable and Sustainable Energy Reviews* 158, article ID 112111. DOI: 10.1016/j.rser.2022.112111
- Parikh, J., Channiwala, S. A., and Ghosal, G. K. (2005). "A correlation for calculating HH-V from proximate analysis of solid fuels," *Fuel* 84(5), 487-494. DOI: 10.1016/j.fuel.-2004.10.010
- Pradhan, P., Mahajani, S. M., and Arora, A. (2018). "Production and utilization of fuel pellets from biomass: A review," *Fuel Processing Technology* 181, 215-232. DOI: 10.1016/j.fuproc.2018.09.021
- Razuan, R., Finney, K. N., Chen, Q., Sharifi, V. N., and Swithenbank, J. (2011). "Pelletised fuel production from palm kernel cake," *Fuel Processing Technology* 92(3), 609-615. DOI: 10.1016/j.fuproc.2010.11.018
- Samuelsson, R., Larsson, S. H., Thyrel, M., and Lestander, T. A. (2012). "Moisture content and storage time influence the binding mechanisms in biofuel wood pellets," *Applied Energy* 99, 109-115. DOI: 10.1016/j.apenergy.2012.05.004
- San Miguel, G., Sánchez, F., Pérez, A., and Velasco, L. (2022). "One-step torrefaction and densification of woody and herbaceous biomass feedstocks," *Renewable Energy* 195, 825-840. DOI: 10.1016/j.renene.2022.06.085
- Sarker, T. R., Nanda, S., Meda, V., and Dalai, A. K. (2023). "Densification of waste biomass for manufacturing solid biofuel pellets: A review," *Environmental Chemistry Letters* 21(1), 231-264. DOI: 10.1007/s10311-022-01510-0
- Searle, S., and Malins, C. (2015). "A reassessment of global bioenergy potential in 2050," *GCB Bioenergy* 7(2), 328-336. DOI: 10.1111/gcbb.12141
- Shang, L., Nielsen, N. P. K., Dahl, J., Stelte, W., Ahrenfeldt, J., Holm, J. K., Thomsen, T., and Henriksen, U. B. (2012). "Quality effects caused by torrefaction of pellets made from Scots pine," *Fuel Processing Technology* 101, 23-28. DOI: 10.1016/j.fuproc.2012.03.013
- Shen, G., Tao, S., Wei, S., Zhang, Y., Wang, R., Wang, B., Li, W., Shen, H., Huang, Y., Chen, Y., *et al.* (2012). "Reductions in emissions of carbonaceous particulate matter and polycyclic aromatic hydrocarbons from combustion of biomass pellets in comparison with raw fuel burning," *Environmental Science and Technology* 46(11), 6409-6416. DOI: 10.1021/es300369d
- Wang, D., Wang, B., and Niu, X. (2014). "Forest carbon sequestration in China and its benefits," *Scandinavian Journal of Forest Research* 29(1), 51-59. DOI: 10.1080/02827581.2013.856936
- Xiao, Z., Yuan, X., Jiang, L., Chen, X., Li, H., Zeng, G., Leng, L., Wang, H., and Huang, H. (2015). "Energy recovery and secondary pollutant emission from the combustion of co-pelletized fuel from municipal sewage sludge and wood sawdust," *Energy* 91, 441-450. DOI: 10.1016/j.energy.2015.08.077
- Yana, S., Nizar, M., Irhamni, and Mulyati, D. (2022). "Biomass waste as a renewable energy in developing bio-based economies in Indonesia: A review," *Renewable and*

- Sustainable Energy Reviews 160, Article ID 112268. DOI: 10.1016/j.rser.2022.112268
- Yin, H., Zhao, W., Li, T., Cheng, X., and Liu, Q. (2018). "Balancing straw returning and chemical fertilizers in China: Role of straw nutrient resources," *Renewable and Sustainable Energy Reviews* 81, 2695-2702. DOI: 10.1016/j.rser.2017.06.076
- Zastempowski, M. (2023). "Analysis and modeling of innovation factors to replace fossil fuels with renewable energy sources Evidence from European Union enterprises," *Renewable and Sustainable Energy Reviews* 178, article ID 113262. DOI: 10.1016/j.rser.2023.113262
- Zhang, R., Shen, G., Zhang, X., Zhang, L., and Gao, S. (2014). "Carbon stock and sequestration of a *Phyllostachys edulis* forest in Changning, Sichuan province," *Acta Ecologica Sinica* 10, article 49. DOI: 10.1186/1471-2296-10-49

Article submitted: June 22, 2024; Peer review completed: July 31, 2024; Revised version received and accepted: August 3, 2024; Published: August 12, 2024. DOI: 10.15376/biores.19.4.7080-7101